Delft University of Technology

Experimental Assessment of the Viability of High Temperature Steam Foam Applications

Jones, Sian; Bos, Robert; Lastovka, Vaclav; Farajzadeh, Rouhi; Riyami, Mohammed

Important note
To cite this publication, please use the final published version (if applicable).
Please check the document version above.

Experimental Assessment of the Viability of High Temperature Steam Foam Applications

Jones, Sian; Bos, Robert; Lastovka, Vaclav; Farajzadeh, Rouhi; Riyami, Mohammed

SPE-200198-MS

Experimental Assessment of the Viability of High Temperature Steam Foam Applications

Sian Jones, Delft University of Technology; Robert Bos, Shell Technology Oman; Vaclav Lastovka, Petroleum Development Oman; Rouhi Farajzadeh, Delft University of Technology; Mohammed Riyami, Petroleum Development Oman

Abstract

The efficiency of oil processes depends on the product of volumetric sweep and microscopic sweep. In oil recovery by steam injection the microscopic sweep is generally good; however, obtaining a good volumetric sweep can be challenging. This is caused by low density and viscosity of the injected steam combined with the reservoir heterogeneity, in particular existence of thief zone. Consequently, the steam utilization factor measured by steam-to-oil ratio (SOR, kg steam/bbl of oil) for many steam-flooding projects becomes poor. All these issues can be addressed by a successful application of steam foam technology.

In steam foam applications, steam (plus a non-condensing gas) is injected simulateneously with a surfactant solution. Under the favorable injection conditions a foam is formed inside the reservoir leading to significant reduction of steam mobility and can eventually improve sweep efficiency.

In the literature many successful steam foam pilots have been reported. However, most of these applications are at relatively shallow reservoirs with low pressures and thus low temperatures. In our paper we investigate if steam foam can also be effectively used for applications at high steam temperatures, significantly exceeding 200°C.

To test the viability of steam foam technology at high temperatures, we have tested the stability of multiple surfactants at reservoir conditions. For those surfactants that showed good stability, core flood tests have been carried out to test the ability to form foam and to assess the resulting foam strength. Steam foam tests have also been carried out at temperature up to 240°C.

Introduction

Steam flooding is a common method for increasing oil recovery in reservoirs with heavy, viscous crudes. The expected recovery factor for the steam flooding process can be expressed as the product of the volumetric sweep efficiency (fraction of the oil-bearing reservoir that is swept by steam) and the microscopic sweep efficiency (fraction of oil recoverd from those parts of the reservoir that have been contacted by steam). While the microscopic sweep efficiency in steam flood is generally good, the volumetric sweep efficiency

can be problematic. Possible reasons for a poor volumetric sweep efficiency in steam flooding are gravity override (steam density is lower than the oil density), viscous fingering due to adverse mobility contrast between steam and heavy oil, and steam channeling through highly permeable streaks in the reservoir.

One possible way to improve the volumetric efficiency in steam flooding is to add a foaming agent to the steam, such that a steam foam forms in the reservoir. Creation of foam will lead to reduction of steam mobility (or increase of its apparent viscosity). Also, it is expeted to form stronger foam in high-permeable (and already swept) layers, and therefore steam can be diverted to the zones with larger oil saturation. The combination of these two effects can eventually help to increase volumetric sweep and thus the expected ultimate recovery in the field (Harasaki, 1989).

Steam foam has been successfully used in several fields in the past (Delamaide, 2016). Most historical applications though have been in relatively shallow reservoirs, with relatively low pressures and thus low steam temperatures. In this paper we will provide results of an experimental lab feasibility study to test the viability of steam foam applications at relatively high temperatures (significantly exceeding 200C). The study contains three main steps. The first step is a bulk foam test, to quickly screen the various surfactant candidates for robust foaming behavior. The second step is a N_2 foam flooding test, where we inject N_2 plus the surfactant mixture into a core to study foaming behavior as a function of gas fraction and temperature. Since we are only coinjecting with N2, the foaming conditions are still relatively favorable. The final test consists of a steam + foam core flood. In this test we co-inject steam (at a chosen steam quality) with and without the surfactant mixture. By studying the difference in pressure drop over the core, we can determine if adding the foaming agent results in the desired foaming behavior.

Materials

Surfactants and Brines
Four different surfactants were considered for testing. These surfactants are proprietary and are therefore identified only as Surfactants A, B, C and D. The brine with composition listed in Table 1, with low TDS (6.69g/litre) was used for all the stability tests carried out. Coreflood tests were carried out using the NaCl brine.

Table 1—Brine recipes

Salt	5 Salt Brine Recipe (g/litre)	NaCl Brine (g/litre)
NaCl	4.851	4.851
NaHCO3	0.964	-
MgCl2. 6H2O	0.293	-
CaCl2.2H2O	0.293	-
NaSO4.10H2O	1.174	-
TDS	6.690	4.851

Rock Samples
An outcrop sandstone rock, Bentheimer, was used for the coreflood experiments. This had a permeability in the range of 0.8-2 D and a porosity of 0.23. Bentheimer has a quartz content of 91.7 wt% and only 2.6 wt% clays (mainly kaolinite) (Peksa et al., 2015)

Experimental Procedures

Thermal Stability of Surfactants

The thermal stability of the surfactants was tested at two temperatures - 250°C and 275°C – and the samples were kept in the oven for time-steps of 1, 2, 4, 8, 16 or 32 days. Surfactant solutions (2 wt% in the 5 salt brine) were placed inside glass sample tubes, which were then placed inside high-pressure sample-tube holders made of stainless steel (Figure 1a). The sample-tube holders were connected together in groups of four (Figure 1b), which allowed four surfactants to be easily tested in parallel. These groups of holders were the placed inside the oven and pressurised to 100 bar prior to heating. For the initial tests, the gas used to pressurise the samples was nitrogen, but it was discovered that this gas dissolved in the surfactant solution at the test pressure. This resulted in outgassing (and hence unwanted foaming) during decompression of the samples at the end of the test. Consequently, later tests were carried out with helium as the pressurising gas.
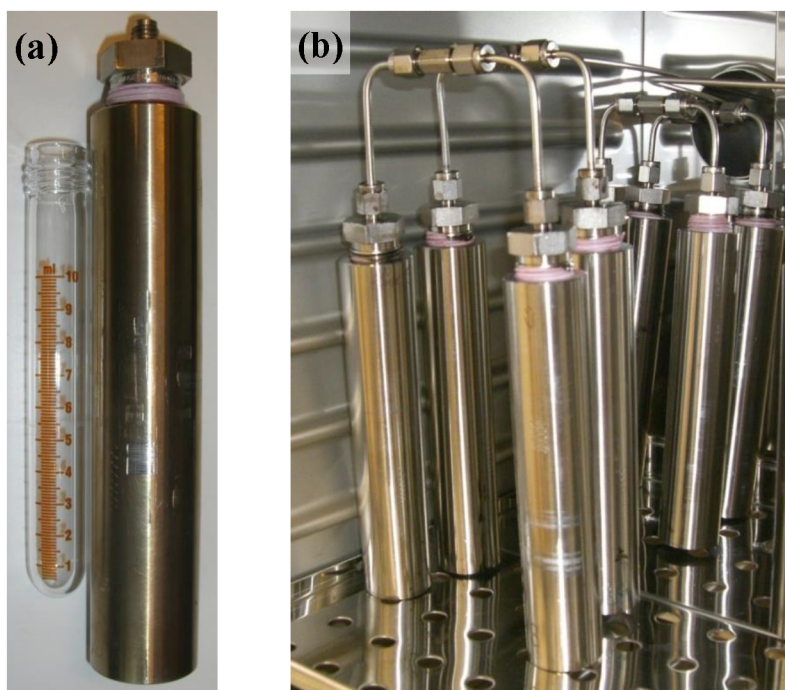
Figure 1—(a) Stainless steel high-pressure sample holder, with glass sample tube. The sealing tape is a copper filled PTFE, which has good temperature resistance. (b) Sample holders inside the oven, connected in groups of four to the 100bar helium supply.

Once samples were removed from the oven, and cooled, they were sealed in the glass sample tubes and posted to the supplying company for analysis of the remaining active matter.

Coreflood Tests with Nitrogen Foam

The coreflood setup was a small-scale setup as previously described (Jones *et al.,* 2016) A schematic diagram of the coreflood set-up is shown in Figure 2. The cores tested were outcrop sandstone rock (Bentheimer), and had a diameter of 0.99 cm and length of 17 cm. This gave a total pore volume of 3.03 cm^3. The sides of the cores were sealed with an epoxy resin (Rencast CW 47, with T_g=210°C, T_g glass transition temperature) before being mounted in aluminium core-holders and glued in position (using R&G MP Advanced resin, with T_g=238°C). The current temperature limit for the coreflood tests (210°C) is determined by the resins used. Once the resin was cured, pressure taps were drilled at two locations along the core (Figure 2), and four absolute pressure gauges connected to the system as indicated. All foam experiments were carried out with a back-pressure of 20 bar.

Figure 2—Schematic diagram of the coreflood setup. To control the temperature, the Bentheimer core is located in an oven.

Solutions with 0.5 wt% surfactant in the 0.48 wt% NaCl brine were coinjected with nitrogen at the base of the core at a constant total flow rate of 0.1 ml/min. This is equivalent to a total superficial velocity, u_t, of 2.15×10^{-5} m/s. Following the results of the stability tests, the surfactants tested in the coreflood setup were B, C, and D.
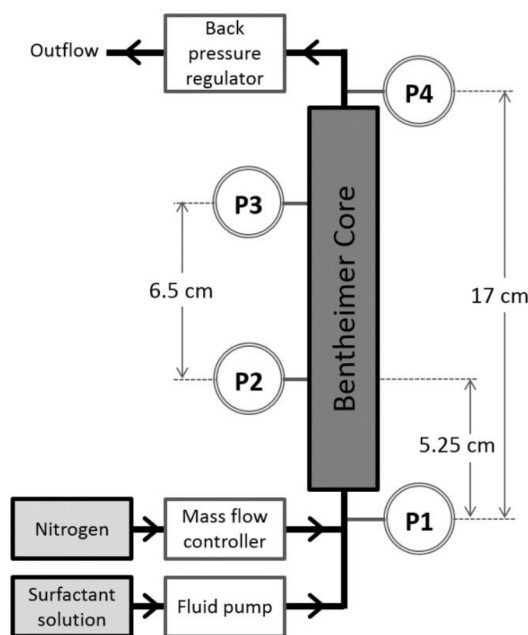
The corefloods were carried out at 60°C, 120°C, 180°C and 210°C. A range of foam qualities (f_g) were injected, where $f_g = u_g/(u_g + u_l)$, and U_g and u_l are the gas and liquid superficial velocities, respectively. The resultant steady-state pressure drop in the core used to calculate the apparent viscosity, μ_{app}, of the foams using Darcy's law:

$$\mu_{app} = \frac{k \nabla p}{u_t},$$

where k is the rock permeability, $u_t\ (=u_g + u_l)$ is the total superficial velocity, and #P is the pressure gradient along the middle of the core (calculated using P2-P3).

Coreflood Tests with Steam Foam

Steam foam tests were carried out in a modified coreflood setup as shown in Figure 3, using the same small-scale Bentheimer core as used for the nitrogen core-floods. The steam generator was placed in the oven along with the core, to minmise heat losses from the steam. Tests were carried out with an oven temperature of 210°C and 240°C. The steam generator temperature could be set independently at a higher value. Thermocouples were placed on the inlet and exit tubing to the core (locations indicated with red dots in Figure 3) to measure the temperature of the fluids at the inlet and outlet. The system pressure was set, via the back-pressure regulator, at value such that the brine or surfactant did evaporate at the oven temperature.
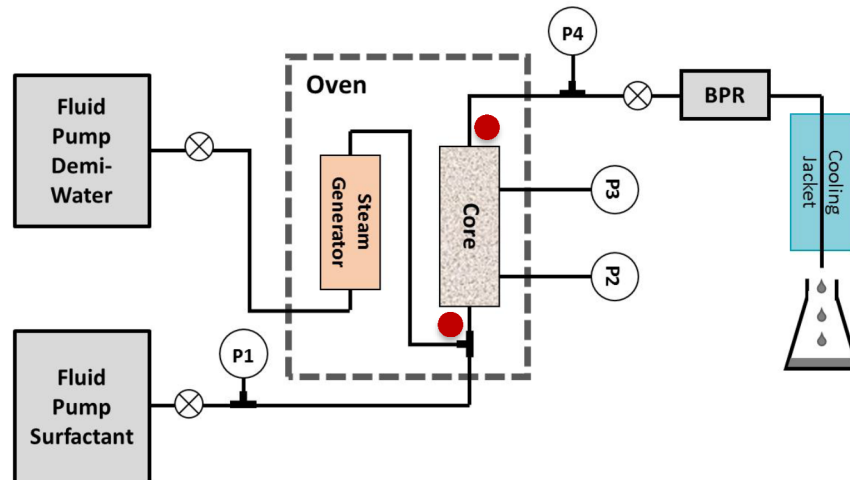
Figure 3—Schematic diagram of the steam foam core-flood setup.

A steam quality of 0.6 was considered for all the tests, with two total flowrates being tested (Table 3). Initial tests were carried out with no foam in the system, co-injecting steam and 0.485wt% NaCl brine to determine the baseline pressure drops along the core. The three pressure drops along the core were considered. The pressure drops are labels as dP_{in}, dP_{mid} and dP_{out}. dP_{in} is calculated as $dP_{in} = P2 - P1$, dP_{mid} is calculated as $dP_{mid} = P3 - P2$ and dP_{out} as $dP_{out} = P4 - P3$. This allowed us to determine the foam strength along the core.

Table 3—Summary of flowrates, temperatures and pressures used for the steam foam tests

Brine/Surfactant Flowrate (ml/min)	Steam Flowrate (CWE) (ml/min)	Oven Temperature (°C)	Steam Generator Temperature (°C)	Back Pressure (bar)
0.83	1.4	210	240	20.5 - 21
		240	290	35-36
1.66	2.8	210	250	20.5 - 21
		240	290	35-36

Following the results of the previous stability and foamability tests, surfactant D was selected for the steam foam tests, in solution with the 0.485wt% NaCl brine. Tests were carried out with a range of different surfactant concentrations: 0.5wt%, 0.1wt%, 0.05wt% and 0.01wt%.

Results and Discussion

Thermal Stability of Surfactants
Typical stability curves, in this case for surfactants A and B, are indicated in Figure 4. The results are standardized using the initial sample concentration. As can be seen, surfactant A showed very good stability at high temperatures (up to the 32 days not shown on graph). For surfactant B, there was reasonable stability at 250°C, with only a 15% drop from the initial value after 8 days. However, once the sample was heated to 275°C it proved to be highly unstable, with 90% of the surfactant degrading within 8 days.
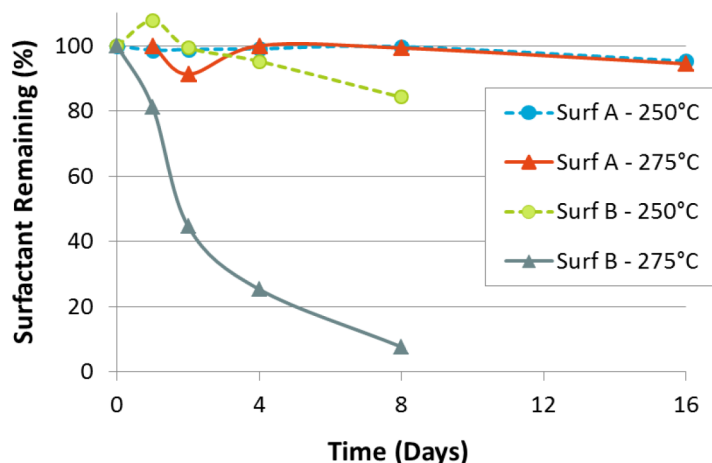
Figure 4—Percentage of surfactant remaining as a function of time, for surfactants A and B at 250°C or 275°C.

Considering the stability results of all the different surfactants, three (A, C and D) were selected for the coreflood tests, to determinc their foaming behaviour

Core Flood Tests – Nitrogen Foam

Coreflood tests were carried out in the outcrop Bentheimer sandstone rock at 60°C, 120°C, 180 °C and 210°C. In these tests we co-inject surfactant mixtures and nitrogen at different foam qualities. The variation in apparent viscosity with foam quality, for solutions of 0.5 wt% surfactants A, C and D in the 0.485wt% NaCl brine, is shown in Figures 5 and 6.

**Figure 5—Variation in apparent viscosity with respect to foam quality at 60°C,
120°C, 180°C and 210°C for (a) surfactant A and (b) surfactant C and c) surfactant D.**

Figure 6—Variation in apparent viscosity, rescaled by the water viscosity at 60°C, 120°C, 180°C and 210°C for (a) surfactant A, (b) surfactant C, c) surfactant D.

It can be seen that, in general, surfactants C and D exhibit similar behavior, with the measured apparent viscosity decreasing as the temperature increases. At the same time, the transition foam quality ($f_g{*}$), where the apparent viscosity 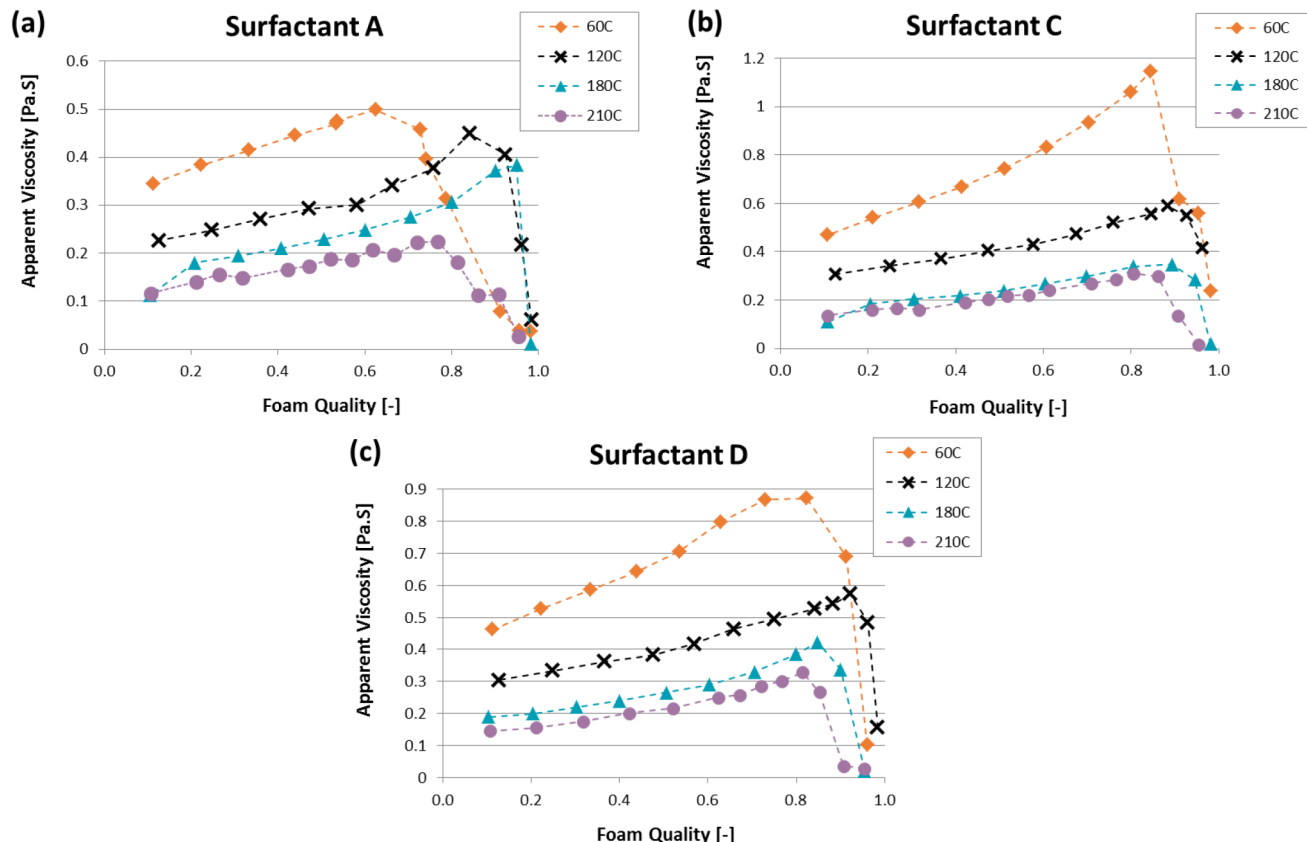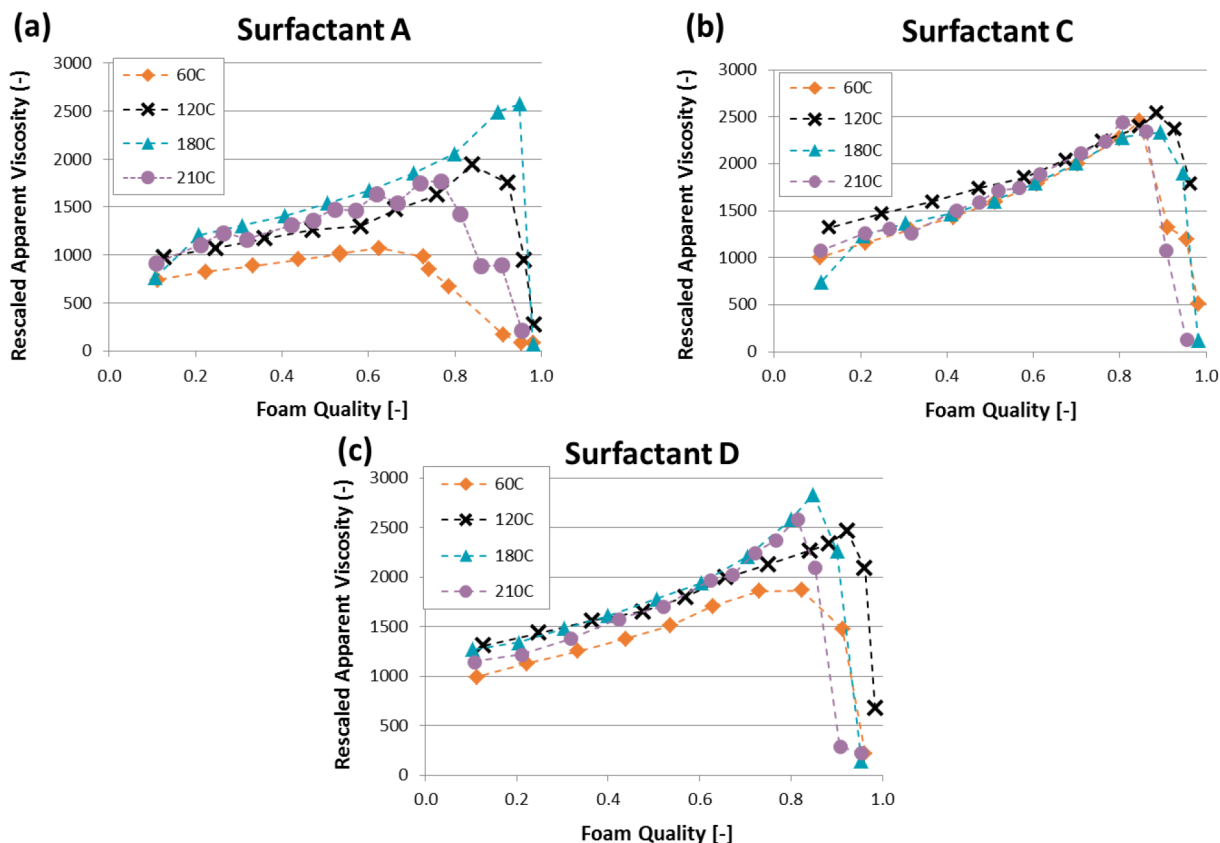is maximum, increases between 60°C and 120°C, before decreasing again at 180°C and 210°C. So the driest foams ($f_g>0.9$) exhibited the strongest behavior at 120°C. The maximum apparent viscosities and the transition foam qualities for each surfactant and temperature are summarized in Table 4.

Table 4—Summary of maximum apparent viscosities and $f_g{*}$ for each surfactant

	Surfactant A		Surfactant C		Surfactant D	
	Maximum Apparent Viscosity (Pa.S)	$f_g{*}$	Maximum Apparent Viscosity (Pa.S)	$f_g{*}$	Maximum Apparent Viscosity (Pa.S)	$f_g{*}$
60°C	0.499	0.62	1.146	0.85	0.872	0.82
120°C	0.449	0.84	0.589	0.88	0.573	0.92
180°C	0.384	0.95	0.348	0.89	0.422	0.85
210°C	0.225	0.77	0.311	0.81	0.329	0.81

The behavior for surfactant A is slightly different, with relatively weak foam (compared to C and D) at 60°C, but with a smaller decrease in the foam strength with increases in temperature. As can be seen in Table

4, the maximum apparent viscosity only decreases slightly between 60°C and 180°C. In this temperature rate the value of f_g^* also increase with temperature.

The reduction in apparent viscosity with increasing temperature was expected, as it was previously observed by Kapetas *et al.* (2016). They attribute this behaviour to a combination of a reduction in the surface tension and visocity of the surfactant solution at higher temperatures. In our case, we have no data on the surface tension of the solutions at the high temperatures, but if we consider rescaling the apparent viscosities by the water viscosity at each test temperature, the curves collapse together as shown in Figure 7. This would indicate that the changing water viscosity is the most important variable at the high temperatures considered. It is also interesting, with the rescaling, that surfactant A shows significantly weaker behavior at 60°C, indicating that this surfactant has been optimized for high temperature use.
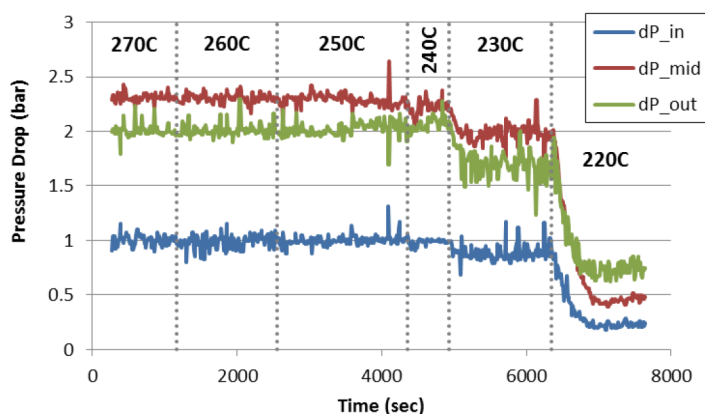

Figure 7—Variation in pressure drops across the core with respect to steam generator temperature. The steam generator temperature was varied from 270°C to 220°C in step of 10°C.

Coreflood Tests – Steam Foam

Baseline tests were carried out to obtain the pressure drops along the core, with no foam in the system, at 210°C and 240°C. Due to thermal losses from the tubing connecting the steam generator to the core (even within the oven), the measured pressure drops were sensitive to the steam-generator temperature. The pressure drops increased with the steam-generator temperature until a steady state was reached (Figure 7). A summary of the steady state behavior used as the baseline for the steam behavior and the corresponding inlet and outlet fluid temperatures are given in Table 5.

Table 5—Summary of the baseline no-foam pressure drops and core inlet and outlet temperatures

Brine Flowrate (ml/min)	Steam Flowrate (CWE) (ml/min)	Oven Temperature (°C)	Steam Generator Temperature (°C)	dP_in (P2-P1) (bar)	dP_mid (P3-P2) (bar)	dP_out (P4-P3) (bar)	T_inlet (°C)	T_outlet (°C)
0.83	1.4	210	240	0.50	1.21	1.04	218.4	214.8
		240	290	0.72	0.94	0.73	244.7	243.3
1.66	2.8	210	250	1.00	2.29	2.02	222.9	215.1
		240	290	1.47	1.78	1.45	248.2	244.2

Steam foam tests were then carried out with surfactant D in 0.485wt% NaCl brine, also at 210°C and 240°C, and with the same two flowrates. Steam foams were generated with surfactant concentrations of 0.5wt%, 0.1wt%, 0.05wt% and 0.01wt%. The pressure drops along the core in the presence of the foam were then compared to the no-foam pressure drops. A summary of the ratios at inlet, mid-section and outlet are given in Figure 8 for the 210°C tests and Figure 9 for the 240°C tests.
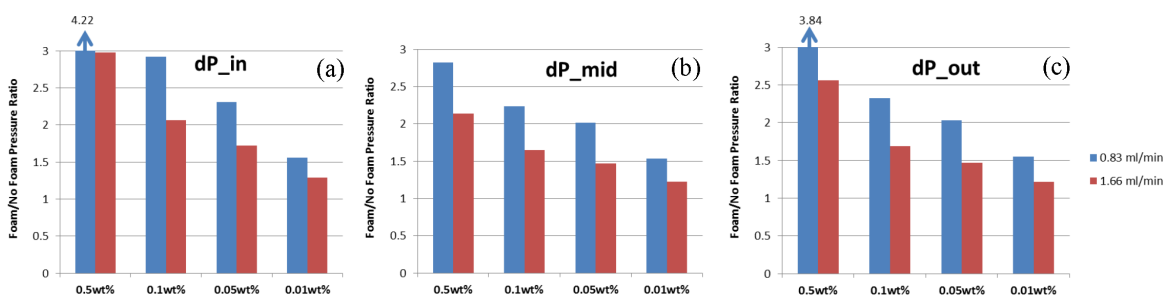
Figure 8—Summary of the Foam/No Foam pressure ratios at 210°C, for varying concentrations of surfactant solution at two different flow rates. The pressure drop ratio was considered for a) dP_in, b) dP_mid and c) dP_out.
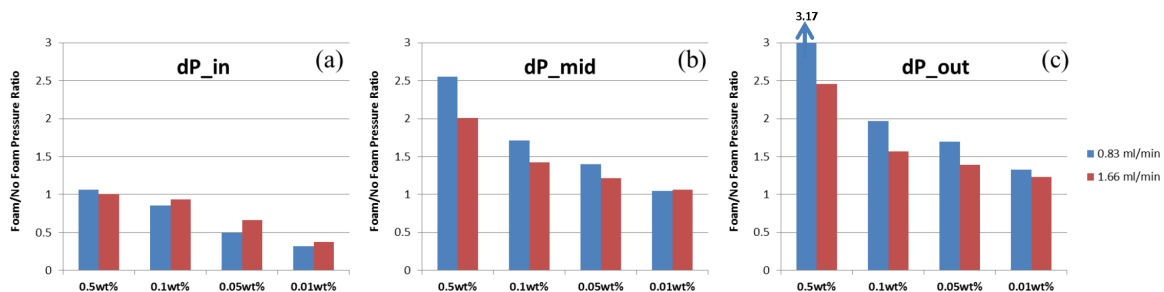

Figure 9—Summary of the Foam/No Foam pressure ratios at 240°C, for varying concentrations of surfactant solution at two different flow rates. The pressure drop ratio was considered for a) dP_in, b) dP_mid and c) dP_out.

At 210°C, the strongest foam strengths were obtained for the highest surfactant concentration, 0.5wt % (Figure 9). However, even at the lowest surfactant concentration, 0.01wt%, a pressure ratio of 1.5 was observed at a surfactant flowrate of 0.83ml/min, indicating that a relatively stable foam was still being generated. The shear thinning behavior of the foam can be seen in the lower pressure ratios seen at the higher flowrate (1.66ml/min of surfactant solution).

Considering dP_out at 240°C, only a small decrease in the foam strength was observed, as compared to the 210°C results, indicating a good temperature response of the foaming behaviour. In comparison, the dP_mid behavior is considerably weaker than at 210°C, and the dP_in pressure ratios would appear to make no sense with values less than 1. It is suggested that both these behaviours are due to degradation of the core, near the inlet injection point, at the high testing temperature, and a micro-CT scan of the inlet confirms this damage (Figure 10) (a more extensive discussion of this problem is given in Appendix A). In this case, the rock is damaged to the extent that a void has been formed, indicating that we are not only observing unconsolidation of the sandgrains in the rock (as discussed in Appendix A), but some grains are being destroyed completely.
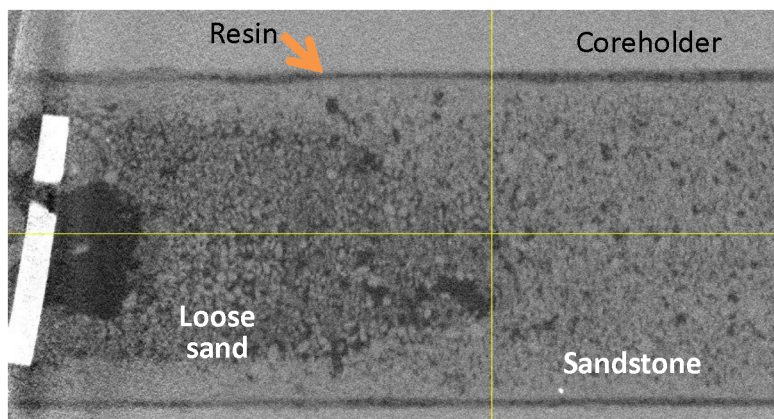
Figure 10—Micro-CT scan of the inlet of the core-plug. The bright line on the left is the titanium frit which helped keep any loose sand grains in place. The region of significantly damaged rock extends approximately 1.5cm into the core.

This degradation causes the permeability of the rock to increase, and hence the measured pressure drop to decrease. This process appears to occur quite rapidly at 240°C, such that some degradation of the core can occur between the no-foam pressure measurements and the foaming tests, resulting in the low values of the pressure ratio. Also, with any degradation of the core, foam generation in this region would also be weaker, again leading to lower pressure drops further along the core. This can also explain the lower pressure drop in dP_mid, as the 'entrance effect' now probably extends into this region of the core. The entrance effect (Ettinger and Radke, 1992) is important in core floods where the surfactant and gas are co-injected, describing the region dominated by foam generation mechanisms near the inlet of the core, before a steady-state foam is achieved. Multiple different factors can affect the length of the entrance effect, and the lower pressure measured at dP_mid could also indicate an increase in the length of the foam generation zone with increasing temperature.

Conclusions

The high-temperature surfactant-screening tests carried out have been useful in identifying the best candidate surfactants for future steam foam tests, and also the ones which are not suitable for work at temperatures over 250°C.

Testing the foamability of the surfactants by carrying out nitrogen foam provided useful information on which surfactant produced the strongest foam, as well as providing useful information on the response to temperature. The temperature response is non-trivial, with all the surfactants showing an increase in f_g^* as the temperature increased from 60°C to 120°C, and surfactant A showing a further increase in f_g^* at 180°C.

Once a surfactant has been shown to generate stable foam with nitrogen at high temperatures, it can then be used to generate a steam foam at elevated temperatures.

For any practical steam foam application, adopting this three-stage process - stability, nitrogen foam, steam foam - can be a useful tool to identify and characterize the optimal surfactant for the particular application.

References

Ettinger, R.A. and Radke, C.J. (1992), Influence of Texture on Steady Foam Flow in Berea Sandstone, *SPE Reservoir Engineering*, **7**, 83–90.

Farajzadeh, R., Lotfollahi, M., Eftekhari, A.A., Rossen, W.R. and Hirasaki, G.J.H. (2015), Effect of permeability on implicit-texture foam model parameters and the limiting capillary pressure, *Energy & fuels*, **29**, 3011–3018.

Jones, S.A., Laskaris, G., Vincent-Bonnieu, S., Farajzadeh, R. and Rossen, W.R. (2016), Effect of surfactant concentration on foam: From coreflood experiments to implicit-texture foam-model parameters, *Journal of Industrial and Engineering Chemistry*, **37**, 268–276.

Kapetas, L., Vincent-Bonnieu, S., Farajzadeh, R., Eftekhari, A.A., Mohd-Shafian, S.R., Bahrim, R.K., & Rossen, W.R. (2015), Effect of permeability on foam-model parameters-an integrated approach from coreflood experiments through to foam diversion calculations, In IOR 2015-18th European Symposium on Improved Oil Recovery.

Kapetas, L., Bonnieu, S.V., Danelis, S., Rossen, W.R., Farajzadeh, R., Eftekhari, A.A. and Bahrim, R.K. (2016), Effect of temperature on foam flow in porous media, *Journal of Industrial and Engineering Chemistry*, **36**, 229–237.

Peksa, A.E., Wolf, K.H.A. and Zitha, P.L. (2015), Bentheimer sandstone revisited for experimental purposes, *Marine and Petroleum Geology*, **67**, 701–719.

Rajapaksha, S., Britton, C., McNeil, R.I., Kim, D.H., Unomah, M., Kulawardana, E. Upamali, N., Weerasooriya, U.P. and Pope, G.A. (2014), Restoration of reservoir cores to reservoir condition before chemical flooding tests. SPE-169887-MS, In SPE Improved Oil Recovery Symposium. *Society of Petroleum Engineers*

Delamaide. (2016). State of the art review of the steam foam process. SPE Latin America and Carribean Heavy and Extra heavy Oil Conference, (SPE 1811160). Lima, Peru.

Harasaki, G. (1989). The steam foam process. *JPT*. 449–456.

Appendix A: Technical Challenges when Testing at High Temperatures

There were several technical challenges encountered during the high temperature tests. The three of most importance are as follows:

1) Great care must be taken when selecting the materials for tubing, connectors and O-rings. In this case, because of the presence of brine and temperatures over 90°C, it was impossible to use stainless steel tubing within the system, and all tubing and connectors was made from Hastelloy. For the O-rings, it was found that several rubber materials that have good temperature resistance, are not stable in wet/steamy environments. The final material chosen for these tests, and which proved reliable, was Kalrez 7375.

2) The selection of the correct resin for sealing the core, then another for gluing the core into the core holder is also technically challenging. The resin that seals the core must be sufficiently viscous that it does not automatically 'wet' the core to a significant depth. This is of a particular importance in 1cm diameter cores, and in the development stage of the project, several promising high temperature resins wetted the cores all the way through, effectively blocking all flow.

3) Of greatest importance, however, is that fact that the continuous flow of surfactant solution at temperatures >200°C cause the cementing minerals in the Bentheimer sandstone to dissolve, results in unconsolidation of the rock core. This typically resulted in about a centimeter of rock at the inlet of the core reverting to sand. Because the core was mounted vertically, this sand could move into the small space created by the presence of the O-ring which rested against the face of the rock. The movement of the sand caused a void to form behind the O-ring (see CT scan of a damaged core in Figure 11), which resulted in the O-ring seal being lost. This quickly led to damage of the resin that glues the core into the core-holder, and the flow then started bypassing the core.
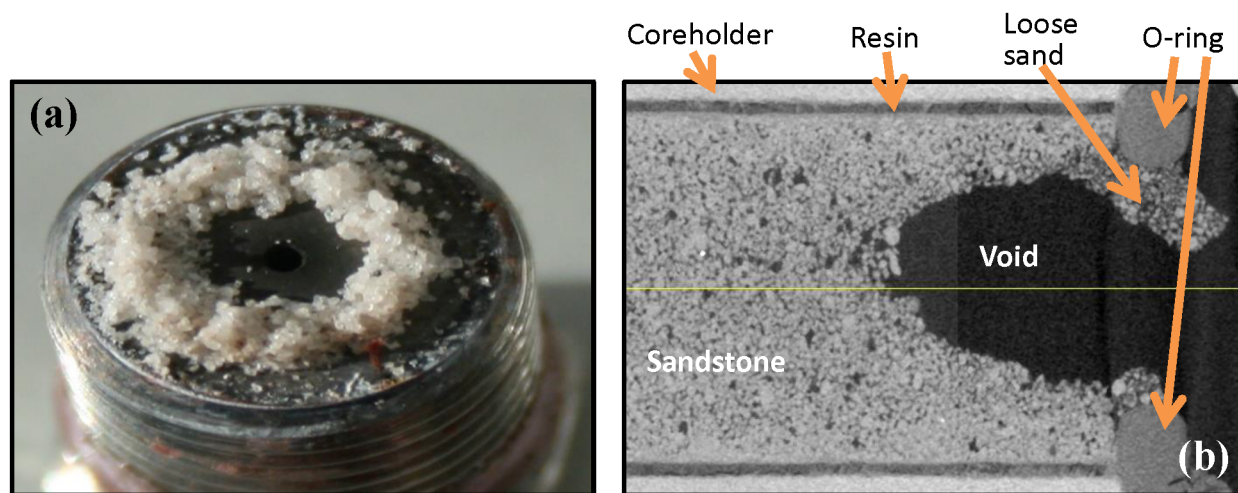

Figure 11—a) Loose sand grains found on the end-cap at the end of a test run, and b) Micro-CT scan of the end of the core, showing the void formed in the rock by the movement of the unconsolidated sand grains.

This problem was partly resolved by placing a small titanium filter in space in the centre of the O-ring. This prevented any of the unconsolidated sand from falling towards the end-cap, reducing the risk of the ring seal being lost and large voids being formed.